DALTON
FULL PAPER

Ruthenium terpyridine complexes incorporating azo-imine based ancillary ligands. Synthesis, crystal structure, spectroelectrochemical properties and solution reactivities †

Biplab Mondal, Mrinalini G. Walawalkar and Goutam Kumar Lahiri *

Department of Chemistry, Indian Institute of Technology, Bombay, Mumbai-400076, India

Received 18th July 2000, Accepted 19th September 2000
First published as an Advance Article on the web 30th October 2000

Ruthenium terpyridine complexes of the type $[Ru^{II}(trpy)(L)(X)][ClO_4]_n$ **1**–**15** [trpy = 2,2′ : 6,2″-terpyridine; L = $NC_5H_4N{=}NC_6H_4(R)$, R = H, *m*-Me, *m*-Cl, *p*-Me or *p*-Cl; X = Cl^-, *n* = 1 (**1**–**5**); H_2O, *n* = 2 (**6**–**10**) or OH^-, *n* = 1 (**11**–**15**)] have been synthesized. The single crystal structures of **1** and **6** were determined. Complex **4** develops in two possible isomeric forms whereas all other complexes stabilise preferentially in one isomeric form. The complexes exhibit strong MLCT bands near 500 nm and ligand based transitions in the UV region. **1**–**5** exhibit moderately strong emissions at 77 K near 600 nm. The chloro (**1**–**5**) and the hydroxo (**11**–**15**) complexes display ruthenium(III)–ruthenium(II) couples and three to four successive one-electron ligand based reductions. The aqua-complexes (**6**–**10**) exhibit a reversible $2e^-/2H^+$ single-step oxidation process in the pH range 1–5.5 corresponding to the $[Ru^{II}(trpy)(L)(H_2O)]^{2+}$–$[Ru^{IV}(trpy)(L)(O)]^{2+}$ couple and the potential decreases linearly with increase in pH. The chemical oxidations of **6**–**10** by an excess of Ce^{IV} in 0.5 M H_2SO_4 also lead to the formation of corresponding $[Ru^{IV}(trpy)(L)(O)]^{2+}$. The oxo-complexes are stable only in the presence of an excess of Ce^{IV}, otherwise they catalyse the oxidation of water to dioxygen and convert back into the parent aqua-species. The pseudo first order rate constant of the process $[Ru^{IV}(trpy)(L)(O)]^{2+} \longrightarrow [Ru^{II}(trpy)(L)(H_2O)]^{2+}$ has been determined.

Introduction

The development of a new class of photo-redox active ruthenium polypyridine complexes has been the subject matter of continuous research activity.[1] Strong metal to ligand charge-transfer transitions, facile electron-transfer properties and long lived ^{3}MLCT excited states of this class of complexes make them effective for designing photochemical and electrochemical devices.[2] In this direction a variety of ruthenium monoterpyridine complexes of the type [Ru(trpy)(L)] (trpy = 2,2′ : 6′,2″-terpyridine) incorporating different kinds of ancillary ligands (L) have been synthesized in recent years.[3] The recent observations of the significant role of ancillary groups (L) in modulating the properties of this class of complexes[4] have initiated the idea of introducing a strong π-acidic azo-imine function $\{NC_5H_4N{=}NC_6H_4(R)\}$ in the [Ru(trpy)] core. This indeed leads to the stepwise syntheses of a series of complexes: $[Ru^{II}(trpy)(L)Cl]^+ \longrightarrow [Ru^{II}(trpy)(L)(H_2O)]^{2+} \longrightarrow [Ru^{II}(trpy)(L)(OH)]^+$ and $[Ru^{II}(trpy)(L)(H_2O)]^{2+} \longrightarrow [Ru^{IV}(trpy)(L)(O)]^{2+}$. Here the chemically generated oxo-complexes are found to be active catalysts for the facile oxidation of water to dioxygen. Herein we report the synthetic aspects, detailed spectroelectrochemical properties of the complexes and the crystal structures of two members of the series (chloro- and aqua-species).

Results and discussion

Synthesis

A group of five azo-imine based ligands L^1–L^5 have been used for the present study. They differ with respect to the location and electronic nature of the 'R' groups present in the pendant phenyl ring. The complexes $[Ru^{II}(trpy)(L)Cl]^+$ **1**–**5** have been synthesized from $[Ru(trpy)Cl_3]$ and L in the presence of NEt_3 and LiCl in refluxing 1 : 1 EtOH–water medium (Scheme 1). The complexes have been isolated as their perchlorate salts and purified by using a silica gel column. The reactions also lead to the formation of *ttt*- and *ctc*-$[Ru^{II}(L)_2Cl_2]$ [*ttt*, *trans-trans-trans*; *ctc*, *cis-trans-cis* with respect to the chlorides, pyridine(N_p) and azo(N_a) nitrogens respectively[5]] as minor by-products (yield: *ttt*, 5–7%; *ctc*, 8–10%). These are separated from the desired complexes (**1**–**5**) by chromatographic techniques (Experimental section).

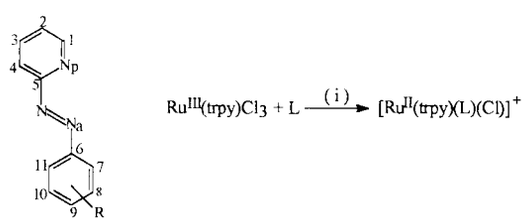

Scheme 1 (i) NEt_3, LiCl, 1 : 1 EtOH–water, heat.

The unsymmetrical nature of L leads to the possibility of two isomers, **A** and **B**, of the complexes **1**–**5**. However, in practice

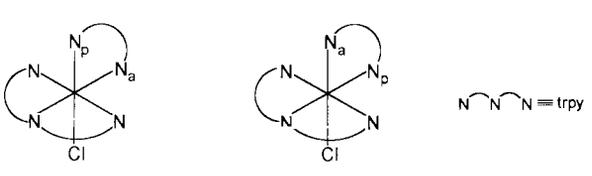

† Electronic supplementary information (ESI) available: micro-analytical and conductivity data for compounds **1**–**15**. See http://www.rsc.org/suppdata/dt/b0/b005789o/

DOI: 10.1039/b005789o

only one has been systematically obtained for **1**–**3** and **5** (see NMR). The crystal structure of **1** establishes the presence of the isomeric form **B** (see later). Since the spectral features of the other complexes (**2**, **3**, **5**) are akin to those of **1** (see later), we therefore logically assume that they also exist in the same isomeric form, **B**.

In the case of complex **4** the solution ^{1}H NMR study indicates the presence of an intimate mixture of both isomers **A** and **B** in a ratio of 1 : 3 (see NMR part). All our attempts to separate the isomers either by column chromatography or by using TLC plates have failed; however, we have succeeded in separating them by a crystallisation technique. Two types of single crystals have been obtained from the bulk; a rectangular type corresponds to isomer **B** and a triangular type **A** (see later). Crystals of specific types were separated carefully and used for further characterisation. Unfortunately they are weakly diffracting and not suitable for structure determination. Efforts to obtain X-ray quality single crystals are in progress. In order to avoid complications due to the presence of isomers in the bulk of **4**, only the crystals corresponding to isomer **B** were used for further studies.

Aqua complexes **6**–**10** have been synthesized in pure state from the corresponding chloro derivatives **1**–**5** by using an excess of $AgNO_3$ in refluxing water medium, eqn. (1). They

$$\underset{\mathbf{1–5}}{[Ru^{II}(trpy)(L)Cl]^+} + AgNO_3 \xrightarrow[\text{heat}]{\text{water}} \underset{\mathbf{6–10}}{[Ru^{II}(trpy)(L)(H_2O)]^{2+}} + AgCl \quad (1)$$

were isolated as their monohydrated perchlorate salts. The conversion of chloro to aqua species has been authenticated by the single crystal structure of **6** (see later). It shows that the isomeric structure **B** of the parent chloro derivative **1** has been retained in the aqua product **6**. The isomeric purity of all the aqua complexes has been confirmed by the ^{1}H NMR technique. Hydroxo complexes **11**–**15** have been prepared from the aqua derivatives **6**–**10** in the presence of alkali as shown in eqn. (2).

$$\underset{\mathbf{6–10}}{[Ru^{II}(trpy)(L)(H_2O)]^{2+}} \xrightarrow[\text{heat}]{\text{NaOH, water}} \underset{\mathbf{11–15}}{[Ru^{II}(trpy)(L)(OH)]^+} \quad (2)$$

The monocationic complexes have been isolated as their monohydrated perchlorate salts. The aqua ⟶ hydroxo conversion is also found to be stereoretentive in nature.

The oxo complexes $[Ru^{IV}(trpy)(L)(O)]^{2+}$ can be generated in solution by chemical oxidation of $[Ru^{II}(trpy)(L)(H_2O)]^{2+}$ **6**–**10** using an excess of Ce^{4+} ion in 0.5 M H_2SO_4. However, they catalyse the oxidation of water to dioxygen and subsequently reduce back to the parent aqua species, a cycle which is repeated on sequential addition of Ce^{4+} (see later). This prevented isolation of the oxo-derivatives in the solid state.

The complexes **1**–**15** are diamagnetic. In acetonitrile solution **1**–**5** and **11**–**15** show 1 : 1 conductivity whereas **6**–**10** behave as 1 : 2 conductors in water. The complexes exhibit satisfactory elemental analyses (ESI).

Crystal structures of $[Ru(trpy)(L^1)Cl]ClO_4$ 1 and $[Ru(trpy)(L^1)(H_2O)][ClO_4]_2\cdot H_2O$ 6

Single crystal structures of the complexes $[Ru(trpy)(L^1)Cl]ClO_4$ **1** and $[Ru(trpy)(L^1)(H_2O)][ClO_4]_2\cdot H_2O$ **6** are shown in Figs. 1 and 2. Selected bond distances and bond angles are given in Table 1. The RuN_5Cl and RuN_5O co-ordination spheres in **1** and **6** respectively are distorted octahedral as can be seen from the angles subtended at the metal ions (Table 1). Terpyridine ligand is co-ordinated in the expected meridional fashion with the ligand L^1 in *cis* orientation.[7] The chloride or the water molecule is *trans* to the azo nitrogen (N_a) of L^1 (structure **B**).

Table 1 Selected bond distances (Å) and angles (°) and their standard deviations for $[Ru(trpy)(L^1)Cl]ClO_4$ **1** and $[Ru(trpy)(L^1)(H_2O)][ClO_4]_2\cdot H_2O$ **6**

1		**6**	
Ru–N(1)	2.070(2)	Ru–N(1)	2.069(6)
Ru–N(2)	1.973(2)	Ru–N(2)	1.967(5)
Ru–N(3)	2.075(2)	Ru–N(3)	2.069(6)
Ru–N(4)	2.055(2)	Ru–N(4)	2.051(5)
Ru–N(6)	1.966(2)	Ru–N(6)	1.944(5)
Ru–Cl	2.408(9)	Ru–O(30)	2.140(5)
N(5)–N(6)	1.304(3)	N(5)–N(6)	1.274(7)
N(6)–Ru–N(2)	101.29(10)	N(6)–Ru–N(2)	96.79(2)
N(6)–Ru–N(4)	76.55(10)	N(6)–Ru–N(4)	76.2(2)
N(2)–Ru–N(4)	176.13(10)	N(2)–Ru–N(4)	172.9(2)
N(6)–Ru–N(1)	87.40(9)	N(6)–Ru–N(1)	90.4(2)
N(2)–Ru–N(1)	79.27(10)	N(2)–Ru–N(1)	79.6(2)
N(4)–Ru–N(1)	103.73(10)	N(4)–Ru–N(1)	99.6(2)
N(6)–Ru–N(3)	96.88(9)	N(6)–Ru–N(3)	96.4(2)
N(2)–Ru–N(3)	79.56(11)	N(2)–Ru–N(3)	78.8(2)
N(4)–Ru–N(3)	97.44(10)	N(4)–Ru–N(3)	102.4(2)
N(1)–Ru–N(3)	158.82(10)	N(1)–Ru–N(3)	157.9(2)
N(6)–Ru–Cl(1)	170.86(7)	N(6)–Ru–O(30)	174.4(2)
N(2)–Ru–Cl(1)	87.01(7)	N(2)–Ru–O(30)	88.3(2)
N(4)–Ru–Cl(1)	95.38(8)	N(4)–Ru–O(30)	98.8(2)
N(1)–Ru–Cl(1)	90.43(7)	N(1)–Ru–O(30)	87.9(2)
N(3)–Ru–Cl(1)	88.34(7)	N(3)–Ru–O(30)	87.1(2)

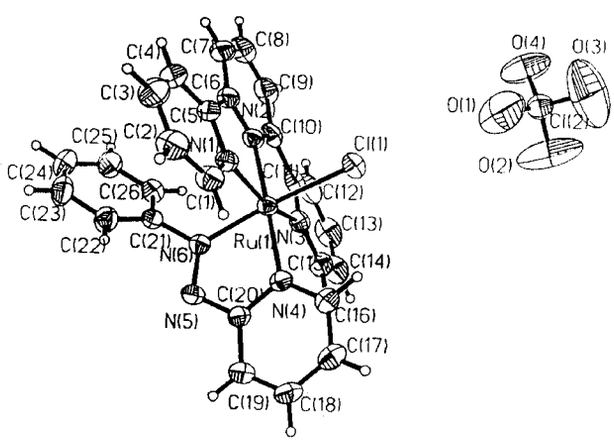

Fig. 1 An ORTEP[6] plot for $[Ru^{II}(trpy)(L^1)Cl]ClO_4$ **1**.

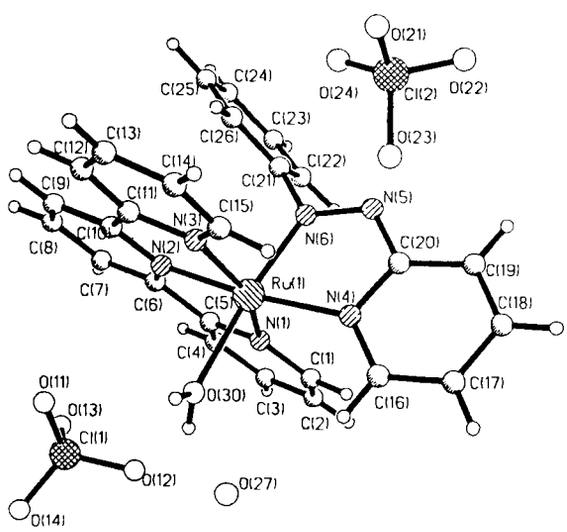

Fig. 2 An ORTEP plot for $[Ru^{II}(trpy)(L^1)(H_2O)][ClO_4]_2\cdot H_2O$ **6**.

The single crystal of **6** contains water of crystallisation in the ratio $[Ru(trpy)(L^1)(H_2O)][ClO_4]_2 : H_2O = 1:1$. The geometrical constraints imposed on the meridional terpyridine ligand are reflected in the *trans* angles, N(1)–Ru–N(3), 158.82(10)° for **1** and 157.9(2)° for **6**. The Ru–N(2) distances (central pyridyl group of terpyridine) in **1** and **6** are approximately 0.1 Å shorter than the terminal Ru–N bonds [Ru–N(1) and Ru–N(3)]. To optimise the chelation of terpyridine, the central Ru–N bond shortens while the terminal one lengthens, which maintains a typical trpy bite angle of ≈ 79°.[3]

The ligand L^1 is bound to the ruthenium ion with the pyridine nitrogen (N_p) and the azo nitrogen (N_a) having a bite angle of 76.55(10)° in complex **1** and 76.2(2)° in **6**. The shorter Ru–N(6) (azo) distances [1.966(2) Å in **1** and 1.944(5) Å in **6**] compared to Ru–N(4)(pyridine) distances [2.055(2) and 2.051(5) Å] of co-ordinated L^1 are due to strong $(d\pi)Ru^{II}\rightarrow\pi^*$(azo) back bonding.[8]

The Ru^{II}–Cl distance, 2.4078(9) Å, in complex **1** is longer than that observed in $[Ru(trpy)(biq)Cl]PF_6$ (biq = 2,2′-biquinoline), 2.378(2) Å,[9] but close to those found in other Ru^{II}–trpy complexes.[10]

The Ru^{II}–$O(H_2O)$ distance, 2.140(5) Å, found in complex **6** is slightly longer than the other known Ru^{II}–$O(H_2O)$ distance, 2.122(16) Å.[11] However, it is much longer than the Ru^{II}–O (phenolato) distances 2.060(3), 2.064(4), 2.022(5) and 2.042(4) Å found in $[Ru^{II}(bpy)_2(Schiff\ base)]^+$,[12] $[Ru^{II}(bpy)_2(pyridine\ phenolate\})]^+$,[13] $[Ru^{II}(pap)_2(catecholate)]$[14] [pap = 2-(phenylazo)pyridine] and $[Ru^{II}(bpy)_2(salicylate)]$[15] complexes respectively.

To the best of our knowledge, this work demonstrates the first crystal structure of an aqua-derivative of ruthenium–terpyridine as well as ruthenium–azopyridine complex systems.

The perchlorate (ClO_4^-) anion is tetrahedral with an average Cl–O distance of 1.363(4) and 1.395(7) Å and an average O–Cl–O angle of 109.416(4) and 109.458(6)° in complexes **1** and **6** respectively.

Spectral properties

There are four notable features in the IR spectra of the complexes. (i) The $\nu_{N=N}$ stretching frequency of the co-ordinated L is appreciably lowered (≈1300 cm^{-1}) compared to that of free L (≈1425 cm^{-1}), evidently due to the $(d\pi)Ru^{II}\rightarrow\pi^*$(L) back bonding effect.[16] (ii) The ν_{Ru-Cl} stretching frequency of **1**–**5** has been observed as a sharp singlet near 320 cm^{-1},[5] which is systematically absent in the spectra of the aqua (**6**–**10**) and hydroxo (**11**–**15**) complexes. (iii) ClO_4^- vibrations are observed near 1100 and 630 cm^{-1}. (iv) The ν_{O-H} vibration for the aqua and hydroxo complexes appeared near 3400 cm^{-1} as expected. The IR spectra of the isomers, **A** and **B**, of **4** are found to be very similar to each other.

^{1}H NMR spectra of the complexes **1**–**5** were recorded in DMSO-d^6 solvent and D_2O was used for the aqua (**6**–**10**) and hydroxo (**11**–**15**) complexes. All three sets of complexes (chloro, aqua and hydroxo) display similar NMR spectra except for the expected changes due to solvent variations. Therefore the data are summarised only for the chloro complexes **1**–**5** (Table 2, Fig. 3). The complexes **1** and **2**–**5** exhibit fifteen and fourteen signals respectively, nine and eight respectively from the non-equivalent L^1 and L^2–L^5 and six from the terpyridine (as the plane of symmetry makes the two halves of terpyridine equivalent).

In the case of complex **4** the aromatic region of the spectrum is complicated due to the presence of two isomers. However, the two well resolved upfield methyl signals at δ 2.17 and 2.15 and direct comparisons of intensities of the individual methyl groups with those of the respective aromatic protons have confirmed the presence of an approximately 1:3 ratio of **A** and **B** isomers in the bulk solution (Fig. 3c). The NMR spectra of the individual isomers **A** and **B** (separated from the crystals) were

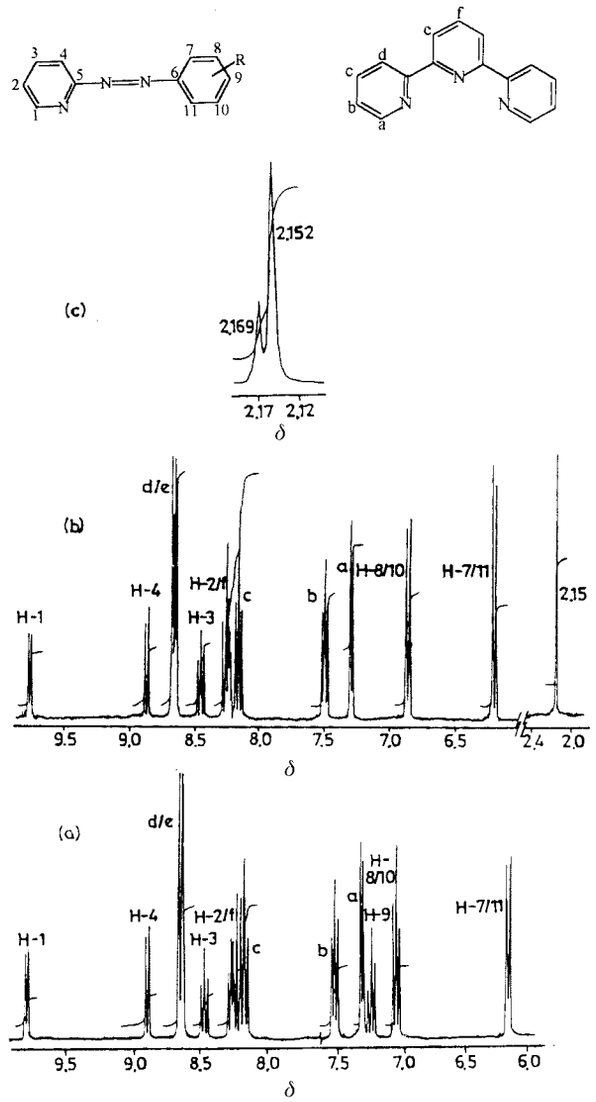

Fig. 3 ^{1}H NMR spectra of (a) $[Ru^{II}(trpy)(L^1)Cl]ClO_4$ **1**, (b) $[Ru^{II}(trpy)(L^4)Cl]ClO_4$ **4** (isomer **B**) and (c) methyl peaks for isomers **A** and **B**.

also recorded and exhibit one distinct methyl signal in each case at the expected positions (δ 2.17 for isomer **A**, 2.15 for **B**). The aromatic region of the spectra exhibit the calculated number of protons corresponding to one particular isomer (Fig. 3b). The methyl signal of complex **2** appears at δ 2.21 as a singlet. The observed signals have been assigned to individual aromatic hydrogens (Table 2) with the aid of ^{1}H NMR correlation spectroscopic (COSY) experiments.[4,5,10,16]

Electronic spectral data of complexes **1**–**15** in dichloromethane solvent are listed in Table 3. In order to study the effect of solvents on the spectral features of the aqua derivatives (**6**–**10**), data were also collected in acetonitrile, methanol and water media (Table 3). Selected spectra are shown in Fig. 4. The complexes display multiple transitions in the UV/visible region. The lowest energy bands near 500 nm are assigned to $(d\pi)Ru^{II}\rightarrow\pi^*$(ligand) metal to ligand charge transfer (MLCT) transitions.[17] Bands in the UV region are believed to be ligand based charge-transfer transitions. Multiple charge transfer transitions may arise from lower symmetry splitting of the metal level, the presence of different acceptor orbitals and from mixing of singlet and triplet configurations in the excited state through spin–orbit coupling.[18] The MLCT band energy follows the order: Cl < OH < H_2O (Table 3, Fig. 4). This red shift in λ_{max} is due to the relative destabilisation of the $(d\pi)$Ru electrons while moving from H_2O to OH to Cl complexes, making the $(d\pi) \longrightarrow \pi^*$ transition occur at relatively lower energy. Elec-

Table 2 ^{1}H NMR spectral data for complexes **1**–**5** in DMSO-d^6

	δ(*J*/Hz)[a]														
	1	2	3	4	7	8	9	10	11	a	b	c	d	e	f
1	9.76 (5.9)[b]	8.25 (6.9)[c] (8.3)	8.46 (6.9)[c] (7.6)	8.90 (6.9)[b]	6.22 (6.8)[b]	7.04 (6.8)[c] (7.7)	7.24 (6.9)[c] (6.9)	7.04 (6.8)[c] (7.7)	6.22 (6.8)[b]	7.31 (5.2)[b]	7.50 (6.9)[c] (6.9)	8.17 (6.9)[c] (6.9)	8.64 (6.8)[b]	8.64 (6.8)[b]	8.22 (7.1)[c] (8.2)
2	9.80 (6.2)[b]	8.22 (8.1)[c] (7.9)	8.51) (6.8)[c] (7.4)	8.84 (7.9)[b]	6.01[d]	Me (2.21)	7.06 (7.3)[b]	6.91 (7.27)[c] (7.63)	6.58 (7.9)[b]	7.34 (6.0)[b]	7.53 (6.3)[c] (5.9)	8.12 (7.1)[c] (7.0)	8.72 (6.7)[b]	8.59 (6.3)[b]	8.20 (6.0)[c] (6.4)
3	9.72 (5.7)[b]	8.24 (7.7)[c] (7.6)	8.42 (8.2)[c] (8.0)	8.91 (7.3)[b]	6.66[d]	Cl	7.61 (6.7)[b]	7.10 (8.2)[c] (7.5)	6.24 (7.3)[b]	7.27 (6.1)[b]	7.76 (7.1)[c] (6.9)	8.14 (7.0)[c] (7.0)	8.70 (6.7)[b]	8.62 (7.0)[b]	8.24 (6.7)[c] (6.7)
4	9.77 (5.5)[b]	8.26 (6.7)[c] (8.5)	8.45 (8.5)[c] (7.7)	8.87 (7.6)[b]	6.19 (8.5)[b]	6.86 (8.5)[b]	Me (2.15)	6.86 (8.5)[b]	6.19 (8.5)[b]	7.29 (5.7)[b]	7.49 (6.7)[c] (8.5)	8.16 (5.7)[c] (5.7)	8.66 (8.5)[b]	8.66 (8.5)[b]	8.22 (5.7)[c] (5.7)
5	9.76 (5.8)[b]	8.29 (7.5)[c] (7.9)	8.45 (6.5)[c] (8.1)	8.93 (8.4)[b]	6.31 (8.2)[b]	7.15 (8.1)[b]	Cl	7.15 (8.1)[b]	6.31 (8.2)[b]	7.29 (6.4)[b]	7.50 (5.8)[c] (5.8)	8.17 (8.2)[c] (8.2)	8.68 (5.0)[b]	8.65 (6.1)[b]	8.27 (8.2)[c] (6.8)

[a] δ and *J* are given in ppm and Hz respectively. Tetramethylsilane is the internal standard. [b] Doublet. [c] Triplet. [d] Singlet.

Table 3 Electronic spectral data

	UV/Vis, λ_{max}/nm (ε/dm^3 mol^{-1} cm^{-1})			
Complex	CH_2Cl_2	CH_3CN	MeOH	Water
1	513(5640), 315(13240), 273(11540), 236(13340)	—	—	—
2	515(11150), 315(26020), 273(24000), 235(27660)	—	—	—
3	515(7510), 314(19220), 273(16730), 232(20210)	—	—	—
4	514(10210), 314(23350), 273(21644), 237(27300)	—	—	—
5	517(5700), 316(14380), 273(12270), 232(16010)	—	—	—
6	494(5600), 332(8170), 311(9200), 270(15400) 228(13990)	493(9650), 327(23410), 282(24350)	490(12100), 332(27100), 281(28000), 270(29000), 226(35100)	487(9830), 330(21270), 308(22430), 270(24760)
7	495(11500), 365(6700), 330(19790), 315(18420), 285(21600), 232(19670)	496(11750), 314(27070), 328(29100), 283(30900)	499(10360), 363(7970), 329(24270), 314(25730), 283(25430), 272(26070)	490(7554), 328(16100), 282(19370), 270(19260)
8	500(10700), 331(24990), 314(25240), 282(25780), 271(25990), 229(27570)	499(7990), 327(20100), 313(18740), 283(20750)	497(7550), 315(19140), 272(19930)	489(8690), 330(18330), 316(17120), 281(20270), 270(20990)
9	495(6601), 384(7730), 331(15800), 284(18000), 272(16700), 232(17000)	490(7950), 375(9460), 329(20390), 282(21490)	495(14710), 377(17530), 330(37490), 272(39170)	490(6500), 379(6390), 329(12980), 281(17580), 271(17840)
10	498(5370), 371(6150), 330(13850), 316(11800), 285(14710), 231(14042)	497(4850), 365(4450), 327(13080), 314(11020), 284(13370), 270(11980)	498(3910), 365(4180), 329(10260), 315(10110), 283(9880), 272(9980)	491(9180), 328(18830), 315(17060), 282(21250), 271(21320)
11	504(6410), 315(17020), 273(23900), 236(22400)	—	—	—
12	505(10890), 312(29100), 272(34000), 230(37000)	—	—	—
13	511(10800), 316(29320), 273(27680), 230(32000)	—	—	—
14	503(11980), 370(16130), 317(33618), 273(36210), 235(44100)	—	—	—
15	512(6200), 316(15840), 273(16050), 230(20740)	—	—	—

tronic spectra of the aqua complexes (**6**–**10**) in co-ordinating solvents, acetonitrile, methanol and water, show little variation (Table 3). The spectra of isomers **A** and **B** of **4** are shown in Fig. 4(c). It seems that they have very similar spectral patterns. In all cases the shift in band maxima based on the 'R' groups present in the framework of L is clear.

The lowest energy MLCT transition of $[Ru(trpy)_2]^{2+}$ appears at 478 nm.[19] Thus the replacement of one strong π-acidic tridentate terpyridine (trpy) ligand by another well known strong π-acidic bidentate azopyridine ligand (L) and one monodentate σ-donor ligand decreases the energy of the same transition. The extent of this decrease essentially depends on the third ligand present in the complex moiety, *i.e.* Cl^-, OH^- or H_2O (Table 3). The overall lowering of the molecular symmetry while moving from $[Ru(trpy)_2]^{2+}$ to the present set of complexes along with the electronic effect of the σ-donor third ligand in the complex moiety might be responsible for the observed trend.[20,21]

Emission properties of complexes **1**–**5** have been studied in optically dilute MeOH–EtOH (1 : 4 v/v) rigid glass at 77 K. Excitations at the top of the lowest energy MLCT band (λ_{max} near 500 nm) exhibit moderately strong emissions near 600 nm

Table 4 Emission data[a]

Compound	λ_{max}/nm excitation	emission	Quantum yield (Φ)
1	506	571	0.72×10^{-2}
2	508	582	0.55×10^{-1}
3	509	589	0.42×10^{-2}
4	510	567	0.98×10^{-2}
5	510	595	0.31×10^{-2}

[a] In ethanol–methanol (4 : 1 v/v) at 77 K.

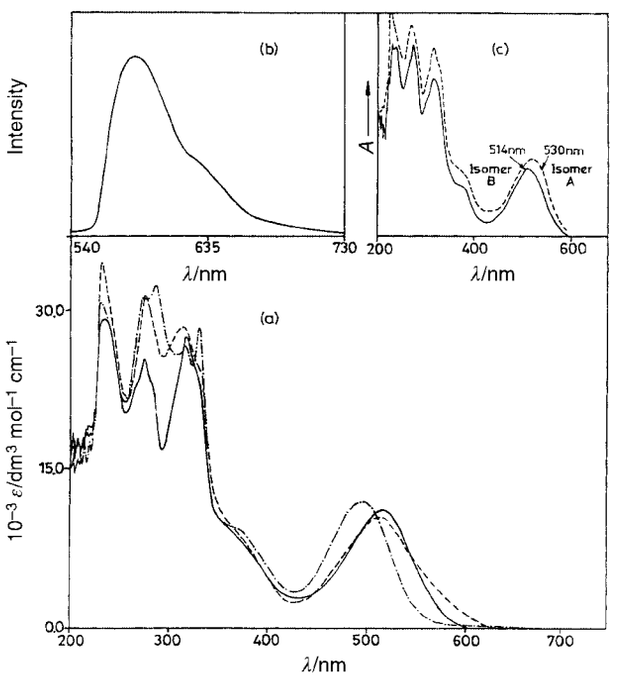

Fig. 4 (a) Electronic spectra of $[Ru^{II}(trpy)(L^2)Cl]ClO_4$ **2** (——), $[Ru^{II}(trpy)(L^2)(OH)]ClO_4$ **12** (----) and $[Ru^{II}(trpy)(L^2)(H_2O)][ClO_4]_2 \cdot H_2O$ **7** (–·–·–) in dichloromethane. (b) Emission spectrum of **2** in EtOH–MeOH 4 : 1 (v/v) at 77 K. (c) Electronic spectra of $[Ru^{II}(trpy)(L^4)Cl]ClO_4$ **4**, isomer **A** (----) and **B** (——), in dichloromethane.

(Table 4, Fig. 4b). The observed emissions are believed to originate from the ^{3}MLCT excited state.[22]

The quantum yields, Φ_{em}, of the emission processes were measured in EtOH–MeOH (4 : 1 v/v) rigid glass at 77 K relative to $[Ru(bpy)_3][PF_6]_2$ for which $\Phi_{em} = 0.35$[23] by following the reported procedure.[24,25] The calculated quantum yields are listed in Table 4 and show reasonable variations depending on the nature of the 'R' functions.

Electron-transfer properties

Redox properties of the chloro (**1**–**5**) and hydroxo (**11**–**15**) complexes have been studied in acetonitrile solvent using a platinum working electrode at 298 K. Representative voltammograms are shown in Fig. 5 and the data are presented in Table 5. All potentials are referenced to the SCE. The complexes **1**–**5** and **11**–**15** display reversible ruthenium(III)–ruthenium(II) couples in the ranges 1.10–1.24 and 0.79–0.92 V respectively.[26] The one-electron nature of the responses is confirmed by constant potential coulometry. Although the oxidised species can be generated by constant-potential coulometry, the oxidised solutions are found to be unstable at room temperature. This prevented isolation of the oxidised species for further characterisation. The formal potential of the ruthenium(III)–ruthenium(II) couple varies depending on the electronic nature and location of the 'R' groups present in L and follows the order **4** < **2** < **1** < **3** < **5** and **14** < **12** < **11** < **13** < **15** for chloro and hydroxo complexes respectively (Table 5). The oxidation of the ruthenium(II) centre for the hydroxo complexes **11**–**15** appears to be relatively easier, which is possibly due to better σ-donor character of the OH function compared to Cl^-. The ruthenium(III)–ruthenium(II) couple of the present set of chloro complexes **1**–**5** is more anodic than that of previously reported analogous complexes, $[Ru^{II}(trpy)(bpy)Cl]^+$[27] and $[Ru^{II}(trpy)(bpz)Cl]^+$[28] (bpy = 2,2′-bipyridine; bpz = 2,2′-bipyrazine). The better π-acidic nature of L compared to bpy and bpz is believed to be the primary contributing factor.[29]

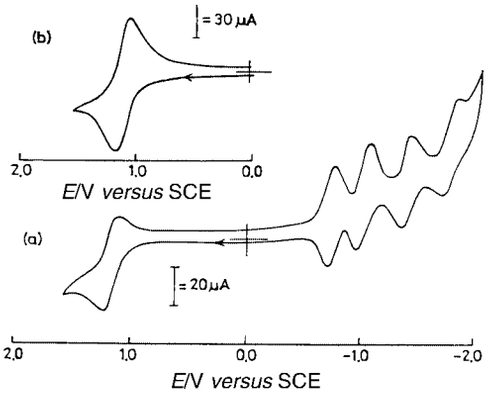

Fig. 5 Cyclic voltammograms of ≈ 10^{-3} mol dm^{-3} solutions of the complexes (a) $[Ru^{II}(trpy)(L^3)Cl]ClO_4$ **3** in acetonitrile and (b) $[Ru^{II}(trpy)(L^3)(H_2O)][ClO_4]_2 \cdot H_2O$ **8** in water at pH 1.0.

The ruthenium(III)–ruthenium(II) couple of $[Ru(trpy)]^{2+}$ appears at 1.30 V.[30] Therefore the potential of this couple decreases while moving from $[Ru(trpy)_2]^{2+}$ to $[Ru(trpy)(L)(X)]^+$. The σ-donor nature of OH^-/Cl^- provides electrostatic stabilisation of the Ru^{III}–L species which has originated from reduction of the overall charge of +2 in $[Ru(trpy)_2]^{2+}$ to +1 in the chloro (**1**–**5**) and hydroxy (**11**–**15**) complexes.

The complexes display three one-electron reductions at negative potentials with respect to the SCE. The one-electron nature of the responses has been established by differential pulse voltammetry, which shows all the reduction waves to have the same height as that of the oxidation wave. Since both the co-ordinating ligands, trpy and L, are known to accept successively two electrons in their lowest unoccupied molecular orbitals,[31] the observed reductions are considered to be ligand based processes. In the case of complexes **3** and **5** (where R = Cl) all the expected four reductions are detected (Fig. 5a). Although there is no direct experimental evidence in favour of assigning the observed reductions corresponding to specific ligands, trpy and L, the first two reductions are assumed to be associated with L. The reductions at the higher potentials are considered to be trpy based processes. The assumption is based on the fact that the azopyridine ligand is known to be a better π acceptor than polypyridyl ligands.[32]

The redox properties of the aqua complexes **6**–**10** have been studied in aqueous media using a platinum working electrode. They behave essentially in a similar manner. In the acidic pH range (0.85–5.5) they show a single-step two-electron oxidation process, Fig. 5(b). The oxidation potentials and the reversibility of the peaks are found to be sensitive to the pH of the medium. At pH > 5.5 the separation between E_{pa} and E_{pc} increases and unfortunately the voltammograms become progressively ill defined in the alkaline pH range, which has precluded electrochemical studies in this range. In the acidic region the potential decreases linearly with increase in pH. The change in oxidation potential as a function of pH is shown in Fig. 6 for a representative case. At pH ≤ 5.5 a shift of peak potentials with pH at the rate of about 60 mV per unit change of pH has been observed (Fig. 6), implying the involvement of a reversible single-step $2e^- + 2H^+$ electrode process, eqn. (3).[28,33] Electro-

Table 5 Electrochemical data at 298 K [a]

Compound	Ru^{III}–Ru^{II} couple E°_{298}/V (ΔE_p/mV)	Ligand reductions E°_{298}/V (ΔE_p/mV)	
		L-based	trpy-based
1	1.15(80)	−0.79(60), −1.41(120)	−1.62(100)
2	1.13(80)	−0.83(60), −1.50(110)	−1.81(100)
3	1.18(90)	−0.72(70), −0.99(100)	−1.38(90), −1.76(120)
4	1.10(100)	−0.77(60), −1.42(90)	−1.75(120)
5	1.24(80)	−0.66(60), −0.95(90)	−1.35(100), −1.65(110)
11	0.84(80)	−0.83(80), −1.49(100)	−1.75(120)
12	0.81(70)	−1.01(90), −1.55(110)	−1.83(130)
13	0.88(90)	−1.00(80), −1.45(120)	−1.70(120)
14	0.79(70)	−0.95(80), −1.58(110)	−1.81(120)
15	0.92(80)	−0.72(70), −1.25(100)	−1.64(110)

[a] Solvent, acetonitrile; supporting electrolyte, $[NBu_4][ClO_4]$; reference electrode, SCE; solute concentration, $\approx 10^{-3}$ M; working electrode, platinum wire. Cyclic voltammetric data: scan rate, 50 mV s^{-1}; $E^\circ_{298} = 0.5(E_{pa} + E_{pc})$ where E_{pa} and E_{pc} are the anodic and cathodic peak potentials, respectively.

Table 6 pK_a values of $[Ru(trpy)(L)(H_2O)]^{2+}$ complexes

Compound	pK_a
6	8.3
7	8.5
8	8.1
9	8.5
10	7.9

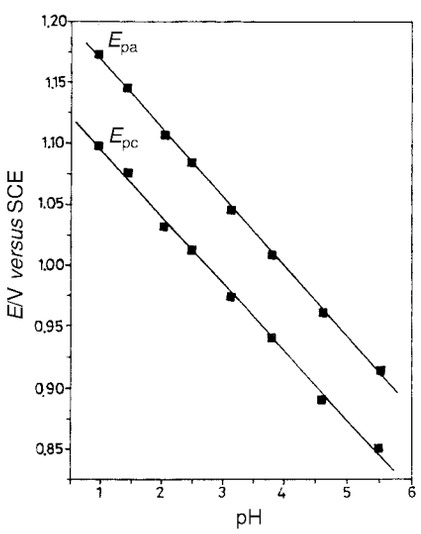

Fig. 6 Variation of cyclic voltammetric peak potentials with pH for $[Ru^{II}(trpy)(L^3)(H_2O)][ClO_4]_2 \cdot H_2O$ **8**.

$$[Ru^{IV}(trpy)(L)(O)]^{2+} + 2H^+ + 2e^- \rightleftharpoons [Ru^{II}(trpy)(L)(H_2O)]^{2+} \quad (3)$$

chemical oxidations of the complexes at a potential greater than the corresponding E_{pa} could not be performed due to continuous coulomb count.[16]

The pK_a values of complexes **6**–**10** have been determined by spectrophotometric titrations using sodium hydroxide (Table 6). The values of similar ruthenium(II) monoterpyridine aqua complexes incorporating bpy, bpz, phen and tmen ancillary ligands (L) are found to be 9.7, 8.8, 9.6 and 10.2 respectively.[28] It may be noted that at acidic pH the analogous bpy system, $[Ru^{II}(trpy)(bpy)(H_2O]^{2+}$, moves to the oxo species $[Ru^{IV}(trpy)(bpy)(O)]^{2+}$ *via* an intermediate species $[Ru^{III}(trpy)(bpy)(OH)]^{2+}$,[27] on the other hand the 2,2′-bipyrazine complex $[Ru^{II}(trpy)(bpz)(H_2O)]^{2+}$ exhibits a one-step $2e^-/2H^+$ transformation to $[Ru^{IV}(trpy)(bpz)(O)]^{2+}$ [28] like the present case. Since the pK_a values of the present set of complexes (7.9–8.5) are closer to that of the bpz complex [$pK_a = 8.8$) and reasonably

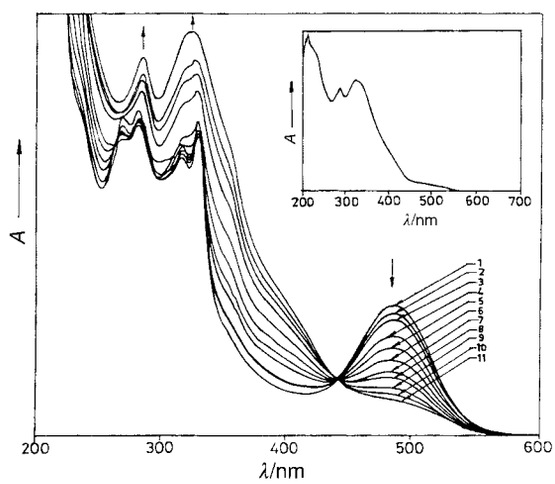

Fig. 7 Change in absorbance of $[Ru^{II}(trpy)(L^4)(H_2O)][ClO_4]_2 \cdot H_2O$ **9** as a function of $[Ce^{IV}]$. Ratio **9**: $[Ce^{IV}]$ = (1) 1:0; (2) 1:0.5; (3) 1:1; (4) 1:2.5; (5) 1:5; (6) 1:10; (7) 1:15; (8) 1:18; (9) 1:25; (10) 1:28; (11) 1:30. Inset shows the spectrum of $[Ru^{IV}(trpy)(L^4)(O)]^{2+}$ obtained separately by using an excess of Ce^{4+}. The arrows indicate increase or decrease in band intensities as the reaction proceeds.

lower than that of the bpy complex ($pK_a = 9.7$), it can be inferred that the acidity of the co-ordinated water molecule or in other words the π-acidic property of the ancillary ligand (L) in the monoterpyridine core is the primary controlling factor in directing the electron-transfer properties of this class of complexes. Thus the strong π acidity of L^{1-5} makes the Ru←OH_2 σ bond correspondingly stronger, which on the other hand facilitates the proton dissociation process.

Chemical oxidation of $[Ru^{II}(trpy)(L)(H_2O)]^{2+}$ by aqueous Ce^{4+} in 0.5 M H_2SO_4: role of $[Ru^{IV}(trpy)(L)(O)]^{2+}$ in catalytic water oxidation

The aqua complexes $[Ru^{II}(trpy)(L)(H_2O)]^{2+}$ **6**–**10** were treated by aqueous cerium(IV) ammonium sulfate at 0.5 M H_2SO_4. This led to an immediate change from red to yellow. In the presence of an excess of Ce^{4+} the MLCT band of $[Ru^{II}(trpy)(L)(H_2O)]^{2+}$ near 500 nm disappears (Fig. 7). It, however, progressively reappears as time passes and eventually attains the initial intensity (Fig. 8). The yellow oxidised solution is found to be stable only in the presence of an excess of Ce^{4+} ion, otherwise it slowly turns back to the parent red aqua species. All our attempts to isolate the oxidised $[Ru^{IV}(trpy)(L)(O)]^{2+}$ complexes have failed altogether as during the work up process they convert back into the aqua derivatives, $[Ru^{II}(trpy)(L)(H_2O)]^{2+}$. Spectrophotometric monitoring of the oxidation of $[Ru^{II}(trpy)(L)(H_2O)]^{2+}$ by using acidic Ce^{4+} solution (0.5 M H_2SO_4) shows the successive development of a new band near 350 nm at the expense of the

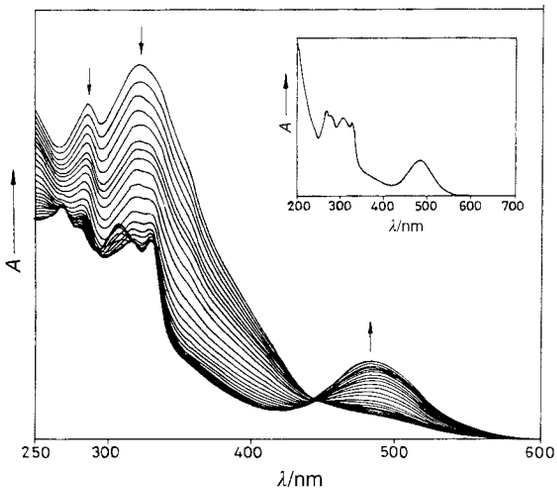

Fig. 8 Time evolution of the electronic spectra of a changing solution of $[Ru^{IV}(trpy)(L^4)(O)]^{2+} \longrightarrow [Ru^{II}(trpy)(L^4)(H_2O)]^{2+}$ in water (0.5 M H_2SO_4) at 303 K. Inset shows the spectrum of pure $[Ru^{II}(trpy)(L^4)(H_2O)]^{2+}$ in water (0.5 M H_2SO_4). Arrows as in Fig. 7.

intense band near 500 nm, characteristic of the starting aqua derivative (Fig. 7). Keeping the electrochemical observation of a single step, $2e^- + 2H^+$ transfer in acidic media (Figs. 5 and 6) in mind, it is logical to consider that in the presence of acidic Ce^{4+} solution the aqua (**6**–**10**) complexes are converted into the oxo-species, eqn. (4). However, the oxo-species further interacts

$$[Ru^{II}(trpy)(L)(H_2O)]^{2+} + 2Ce^{4+} \longrightarrow [Ru^{IV}(trpy)(L)(O)]^{2+} + 2Ce^{3+} + 2H^+ \quad (4)$$

with the solvent water and converts back into the parent aqua derivative (eqn. 5).

$$[Ru^{IV}(trpy)(L)(O)]^{2+} + H_2O \longrightarrow [Ru^{II}(trpy)(L)(H_2O)]^{2+} + \tfrac{1}{2}O_2 \quad (5)$$

The backward reduction process (eqn. 5) has been followed spectrophotometrically with time (Fig. 8). The decrease in intensity of the band near 350 nm, characteristic of the oxo-species with concomitant growth of a new band near 500 nm, characteristic of the aqua complex (Fig. 8), reveals the active role of $[Ru^{IV}(trpy)(L)(O)]^{2+}$ species in oxidising the water molecules (eqn. 5). However, sequential additions of acidic Ce^{4+} to the reaction mixture essentially repeat the process, eqns. (4) and (5), The overall process is therefore catalytic in nature, Scheme 2. The progressive accumulation of dioxygen in such

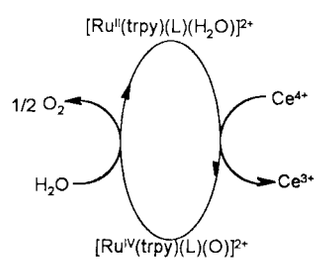

Scheme 2

solutions is established with the help of the observed reduction peak of $O_2 + e^- \longrightarrow O_2^-$ at −0.3 V.[34] However, whether the dioxygen is formed directly or *via* the intermediacy of H_2O_2 is still not clear.

The pseudo first order rate constant (k) of reaction (5) has been determined spectrophotometrically for all the complexes (Fig. 8, Table 7). The rate constant of the conversion process $[Ru^{IV}(trpy)(L)(O)]^{2+} \longrightarrow [Ru^{II}(trpy)(L)(H_2O)]^{2+}$ is found to vary systematically depending on the electronic nature of the ancillary ligand moiety (L).

Table 7 Pseudo first order rate constants (k) for the conversion $[Ru^{IV}(trpy)(L)(O)]^{2+} \longrightarrow [Ru(trpy)(L)(H_2O)]^{2+}$ in aqueous acidic media at 298 K

Compound	$10^3\ k/s^{-1}$
$[Ru^{IV}(trpy)(L^1)(O)]^{2+}$	7.6
$[Ru^{IV}(trpy)(L^2)(O)]^{2+}$	6.8
$[Ru^{IV}(trpy)(L^3)(O)]^{2+}$	8.2
$[Ru^{IV}(trpy)(L^4)(O)]^{2+}$	7.1
$[Ru^{IV}(trpy)(L^5)(O)]^{2+}$	8.8

Conclusion

The role of azo-imine based strong π-acidic ancillary ligands L^{1-5} in the ruthenium monoterpyrdine [Ru(trpy)] core has been scrutinised with particular reference to the spectroelectrochemical properties of this class of complexes. Thus series of complexes $[Ru^{II/III}(trpy)(L)Cl]^{+/2+}$ **1**–**5**, $[Ru^{II}(trpy)(L)(H_2O)]^{2+}$ **6**–**10**, $[Ru^{II}(trpy)(L)(OH)]^+$ **11**–**15** and $[Ru^{IV}(trpy)(L)(O)]^{2+}$ have been synthesized and studied. Their properties have been compared with those of similar complexes incorporating L = bpy and bpz. In the case of bpy the aqua-complex $[Ru(trpy)(L)(H_2O)]^{2+}$ undergoes stepwise $1e^-/1H^+$ oxidations $Ru^{II}(H_2O) \longrightarrow Ru^{III}(OH) \longrightarrow Ru^{IV}(O)$; where L = 2,2′-bipyrazine, there is a one step $2e^-/2H^+$ transformation, $Ru^{II}(H_2O) \longrightarrow Ru^{IV}(O)$, whereas in the present case ($L = L^{1-5}$) the complexes **6**–**10** not only display one step $2e^-/2H^+$ oxidation, $Ru^{II}(H_2O) \longrightarrow Ru^{IV}(O)$, but the resultant oxo-species also catalyse water oxidation. The stronger acidity of the co-ordinated water molecule ($pK_a \approx 8.0$) as well as the higher oxidation potential (>1.1 V) of $[Ru(trpy)(L^{1-5})(H_2O)]^{2+}$ compared to those of the complexes where L = bpy or bpz possibly make the oxo-species of the present set of complexes, $[Ru(trpy)(L^{1-5})(O)]^{2+}$, effective in catalysing the oxidation of water to dioxygen. Thus the present study implies a role for the electronic aspects of the ancillary ligands L in the physico-chemical properties of the monoterpyridine complexes. The complexes **1**–**5** are found to exhibit moderately strong emissions at 77 K. Further reactivity studies of the aqua- and oxo-complexes are in progress.

Experimental

Materials

Commercial ruthenium trichloride (S.D. Fine Chemicals, Bombay, India) was converted into $RuCl_3 \cdot 3H_2O$ by repeated evaporation to dryness with concentrated hydrochloric acid. The complex $[Ru(trpy)Cl_3]$ and the ligands L^{1-5} were prepared according to the reported procedures.[3,35] 2,2′:6,2″-Terpyridine was obtained from Aldrich, USA. Other chemicals and solvents were reagent grade and used as received. Silica gel (60–120 mesh) used for chromatography was of BDH quality. For spectroscopic and electrochemical studies HPLC grade solvents were used. Water of high purity was obtained by distillation of deionised water from $KMnO_4$. Sodium perchlorate for electrochemical work in aqueous media was recrystallised from water.

Physical measurements

UV-visible spectra were recorded by using a Shimadzu-2100 spectrophotometer, FT-IR spectra on a Nicolet spectrophotometer with samples prepared as KBr pellets. Solution electrical conductivity was checked using a Systronic 305 conductivity bridge. Magnetic susceptibility was checked with a PAR vibrating sample magnetometer. NMR spectra were obtained with a 300 MHz Varian FT spectrometer. Cyclic voltammetric, differential pulse voltammetric and coulometric measurements were carried out using a PAR model 273A electrochemistry system. Platinum wire working and auxiliary electrodes and an aqueous saturated calomel reference

electrode were used in a three electrode configuration. The supporting electrolyte was NBu_4ClO_4 and the solute concentration was $\approx 10^{-3}$ M. The half-wave potential E°_{298} was set equal to $0.5(E_{pa} + E_{pc})$, where E_{pa} and E_{pc} are anodic and cathodic cyclic voltammetric peak potentials respectively. A platinum wire-gauze working electrode was used in coulometric experiments. All experiments were carried out under a dinitrogen atmosphere and were not corrected for junction potentials. The elemental analyses were carried out with a Carlo Erba (Italy) elemental analyser. Solution emission properties were checked using a SPEX-fluorolog spectrofluorometer.

Kinetic measurements

The conversion $[Ru^{IV}(trpy)(L)(O)]^{2+} \longrightarrow [Ru^{II}(trpy)(L)(H_2O)]^{2+}$ was monitored spectrophotometrically. For the determination of k the increase in absorption (A_t) at 480 nm corresponding to the aqua-species was recorded as a function of time (t). A_∞ was measured when the intensity changes levelled off. Values of pseudo first order rate constants, k, were obtained from the slopes of linear least-squares plots of $-\ln(A_0 - A_t)$ against t.[36]

Preparation of complexes

The complexes $[Ru(trpy)(L^{1-5})Cl]ClO_4$ **1**–**5** were synthesized by following a general procedure. Yields vary in the range 70–75%. Details are given for one representative complex **2**.

$[Ru(trpy)(L^2)Cl]ClO_4$ 2. A 100 mg (0.227 mmol) quantity of $[Ru(trpy)Cl_3]$ was taken in 1:1 ethanol–water (25 ml) and heated at reflux for 5 min. The ligand L^2 (44.73 mg, 0.227 mmol) followed by LiCl (100 mg) and NEt_3 (1.5 ml) were added to the hot solution and the mixture was heated to reflux for 5 h. The solvent was then removed under reduced pressure. The dry mass was dissolved in the minimum volume of acetonitrile and to it was added a saturated aqueous solution of $NaClO_4$ (3 ml). The mixture was kept in a refrigerator overnight. The crystalline mass thus obtained was filtered off, washed with a little ice-cold water and dried *in vacuo* over P_4O_{10}. The dried product was purified by using a silica gel column. With dichloromethane–acetonitrile (5:1) a blue solution corresponding to *ctc*-$[Ru(L^2)_2Cl_2]$ was separated initially; *ttt*-$[Ru(L^2)_2Cl_2]$ was eluted next by dichloromethane–acetonitrile (4:1). Using dichloromethane–acetonitrile (2:1) as eluent a red band corresponding to the desired product $[Ru(trpy)(L^2)Cl]ClO_4$ **2** was separated and collected. Evaporation of the solvent under reduced pressure afforded a pure solid. Yield: 106 mg (70%).

The aqua-complexes $[Ru(trpy)(L)(H_2O)][ClO_4]_2\cdot H_2O$ **6**–**10** were prepared from the corresponding chloro-derivatives **1**–**5** using aqueous $AgNO_3$. Details are mentioned for one complex **7**.

$[Ru(trpy)(L^2)(H_2O)][ClO_4]_2\cdot H_2O$ 7. The chloro complex $[Ru(trpy)(L^2)Cl]ClO_4$ **2** (100 mg, 0.15 mmol) was taken in 20 ml water and to it an excess of $AgNO_3$ (102 mg, 0.6 mmol) was added. The mixture was heated to reflux for 2 h, then kept in a refrigerator for 1 h. The precipitated AgCl was separated by filtration through a sintered glass crucible (G-4). The volume of the filtrate was then reduced to 5 ml and saturated aqueous $NaClO_4$ solution added. The solution was kept in the refrigerator overnight. The precipitate of the aqua-species **7** thus obtained was filtered off, washed with ice-cold water and dried *in vacuo* over P_4O_{10}. Yield: 73 mg, 65%.

The complexes $[Ru(trpy)(L)(OH)]ClO_4\cdot H_2O$ **11**–**15** were prepared from the corresponding aqua-derivatives **6**–**10** in the presence of NaOH. Details are given for one complex **12**.

$[Ru(trpy)(L^2)(OH)]ClO_4\cdot H_2O$ 12. The aqua-complex $[Ru(trpy)(L^2)(H_2O)][ClO_4]_2\cdot H_2O$ (100 mg, 0.13 mmol) was dissolved in 25 ml water and 10 ml of aqueous NaOH (20 mg, 0.5 mmol) were added dropwise. The mixture was stirred magnetically at room temperature. The orange colour of the aqua derivative gradually changed to pink. Stirring was continued for 1 h. The volume of the solution was reduced over a water bath and a saturated aqueous solution of $NaClO_4$ was added to the cold solution. The dark coloured solid mass thus obtained was filtered off, washed with ice-cold water and dried *in vacuo* over P_2O_5. Yield: 67.5 mg, 80%.

Table 8 Crystallographic data for $[Ru(trpy)(L^1)Cl]ClO_4$ **1** and $[Ru(trpy)(L^1)(H_2O)][ClO_4]_2\cdot H_2O$ **6**

	1	**6**
Formula	$C_{26}H_{20}Cl_2N_6O_4Ru$	$C_{26}H_{24}Cl_2N_6O_{10}Ru$
M	652.45	752.48
Crystal symmetry	Monoclinic	Monoclinic
Space group	$P2_1/n$	$P2_1/n$
a/Å	8.598(18)	9.297(9)
b/Å	15.974(3)	16.402(9)
c/Å	19.496(5)	20.110(15)
β/°	99.388(18)	103.076(7)
V/Å^3	2642.1(0)	2987(4)
Z	4	4
μ/mm^{-1}	0.841	0.770
$R1$	0.030	0.052
$wR2$	0.079	0.095
Measured/unique reflections [R_{int}]	4922/4640 [0.0108]	5392/5326 [0.0283]

Crystallography

Single crystals of the complexes were grown by slow diffusion of an acetonitrile solution of **1** in benzene followed by slow evaporation, and slow evaporation of an aqueous solution of **6** respectively. Significant crystal data and data collection parameters are listed in Table 8. Absorption correction was done by performing psi-scan measurement.[37] The data reduction was done by using MAXUS and structure solution and refinement using the programs SHELXS 97 and SHELXL 97 respectively.[38] The metal atom was located from the Patterson map and the other non-hydrogen atoms emerged from successive Fourier synthesis. The structures were refined by full-matrix least squares on F^2. All non-hydrogen atoms were refined anisotropically. Hydrogen atoms were included in calculated positions. The difference map revealed the presence of one molecule of lattice water in **6**.

CCDC reference number 186/2186.

See http://www.rsc.org/suppdata/dt/b0/b005789o/ for crystallographic files in .cif format.

Acknowledgements

Financial support received from the Department of Science and Technology, New Delhi and Council of Scientific and Industrial Research, New Delhi, India, is gratefully acknowledged. The X-ray structural studies were carried out at the National Single Crystal Diffractomer Facility, Indian Institute of Technology, Bombay. Special acknowledgement is made to Regional Sophisticated Instrumental Center, RSIC, Indian Institute of Technology, Bombay for providing the NMR facility.

References

1 V. Balzani and F. Scandola, *Supramolecular Photochemistry*, Horwood, Chichester, 1991; K. Kalyanasundaram, *Coord. Chem. Rev.*, 1989, **28**, 2920; T. J. Meyer, *Pure Appl. Chem.*, 1986, **58**, 1193.

2 F. Scandola, C. A. Bignozzi and M. T. Indelli, *Photosensitization and Photocatalysis Using Inorganic and Organometallic Compounds*, eds. K. Kalyanasundaram and M. Gratzel, Kluwer, Dordrecht, 1993, p. 161.

3 B. Mondal, S. Chakraborty, P. Munshi, M. G. Walawalkar and G. K. Lahiri, *J. Chem. Soc., Dalton Trans.*, 2000, 2327; K. Hutchison, J. C. Morris, T. A. Nile, J. L. Walsh, D. W. Thompson,

J. D. Petersen and J. R. Schoonover, *Inorg. Chem.*, 1999, **38**, 2516; J. Zadykowicz and P. G. Potvin, *Inorg. Chem.*, 1999, **38**, 2434; R. M. Berger and D. R. McMillin, *Inorg. Chem.*, 1998, **27**, 4245; R. R. Ruminski, S. Underwood, K. Vallely and S. J. Smith, *Inorg. Chem.*, 1998, **37**, 6528; E. C. Constable, C. J. Cathey, M. J. Hannon, D. A. Tocher, J. V. Walker and M. D. Ward, *Polyhedron*, 1998, **18**, 159; J. P. Sauvage, J. P. Collin, J. C. Chambron, S. Guillerez, C. Coudret, V. Balzani, F. Barigelletti, L. De Cola and L. Falmigni, *Chem. Rev.*, 1994, **94**, 993; A. Pramanik, N. Bag and A. Chakravorty, *J. Chem. Soc.*, *Dalton Trans.*, 1992, 97; C. A. Howard and M. D. Ward, *Angew. Chem.*, *Int. Ed. Engl.*, 1992, **31**, 1028; B. P. Sullivan, J. M. Calvert and T. J. Meyer, *Inorg. Chem.*, 1980, **19**, 1404.

4 T. Wada, K. Tsuge and K. Tanaka, *Angew. Chem.*, *Int. Ed.*, 2000, **39**, 1479; A. El-ghayoury, A. Harriman, A. Khatyr and R. Ziessel, *Angew. Chem.*, *Int. Ed.*, 2000, **39**, 185; K. Tsuge and K. Tanaka, *Chem. Lett.*, 1998, 1069; M. Kurihara, S. Daniele, K. Tasuge, M. Sugimoto and K. Tanaka, *Bull. Chem. Soc. Jpn.*, 1998, **71**, 867; A. Doveletoglou, S. A. Adeyemi and T. J. Meyer, *Inorg. Chem.*, 1996, **35**, 4120; S. C. Rasmussen, S. E. Ronco, D. A. Mlsna, M. A. Billadeau, W. T. Pennington, J. W. Kolis and J. D. Petersen, *Inorg. Chem.*, 1995, **34**, 821; A. Lobet, P. Doppelt and T. J. Meyer, *Inorg. Chem.*, 1988, **27**, 514.

5. P. Munshi, R. Samanta and G. K. Lahiri, *Polyhedron*, 1998, **17**, 1913.

6 C. K. Johnson, ORTEP II, Report ORNL-5138, Oak Ridge National Laboratory, Oak Ridge, TN, 1976.

7 A. Spek, A. Gerli and J. Reedjik, *Acta Crystallogr.*, *Sect. C*, 1994, **50**, 394; N. Grover, N. Gupta, P. Singh and H. H. Thorp, *Inorg. Chem.*, 1992, **31**, 2014; N. C. Pramanik, K. Pramanik, P. Ghosh and S. Bhattacharya, *Polyhedron*, 1998, **17**, 1525.

8 B. K. Santra, G. A. Thakur, P. Ghosh, A. Pramanik and G. K. Lahiri, *Inorg. Chem.*, 1996, **35**, 3050.

9 A. E. M. Boelrijk and J. Reedijk, *J. Mol. Catal.*, 1994, **89**, 63.

10 C. J. Cathey, E. C. Constable, M. J. Hannon, D. A. Tocher and M. D. Ward. *J. Chem. Soc.*, *Chem. Commun.*, 1990, 621; R. J. Forster, A. Boyle, J. G. Vos, R. Hage, A. H. J. Dijkhuis, R. A. G. DeGraff, J. G. Haasnoot, R. Prins and J. Reedijk, *J. Chem. Soc.*, *Dalton Trans.*, 1990, 121; J. M. Clear, J. M. Kelley, C. M. O'Connell, J. G. Vos, C. J. Cardin, S. R. Costa and A. J. Edwards, *J. Chem. Soc.*, *Chem. Commun.*, 1980, 750.

11 P. Bernhard, H. B. Burgi, J. Hauser, H. Lehmann and A. Ludi, *Inorg. Chem.*, 1982, **21**, 3936.

12 S. Chakraborty, M. G. Walawalkar and G. K. Lahiri, *J. Chem. Soc.*, *Dalton Trans.*, 2000, 2875.

13 B. M. Holligan, J. C. Jeffery, M. K. Norgett, E. Schatz and M. D. Ward, *J. Chem. Soc.*, *Dalton Trans.*, 1992, 3345.

14 N. Bag, A. Pramanik, G. K. Lahiri and A. Chakravorty, *Inorg. Chem.*, 1992, **31**, 40.

15 V. R. L. Constantino, H. E. Toma, L. F. C. de Oliveira, F. N. Rein, R. C. Rocha and D. O. Silva, *J. Chem. Soc.*, *Dalton Trans.*, 1999, 1735.

16 B. K. Santra and G. K. Lahiri, *J. Chem. Soc.*, *Dalton Trans.*, 1997, 129.

17 D. A. Bardwell, A. M. W. Cargill Thompson, J. C. Jeffery, J. A. McCleverty and M. D. Ward, *J. Chem. Soc.*, *Dalton Trans.*, 1996, 873.

18 E. M. Kober and T. J. Meyer, *Inorg. Chem.*, 1982, **21**, 3967; B. J. Pankuch, D. E. Lacy and G. A. Crosby, *J. Phys. Chem.*, 1980, **84**, 2061; A. Ceulemans and L. G. Vanquickenberne, *J. Am. Chem. Soc.*, 1981, **103**, 2238.

19 C. R. Hecker, A. K. I. Gushurst and R. D. McMillin, *Inorg. Chem.*, 1991, **30**, 538.

20 B. K. Santra and G. K. Lahiri, *J. Chem. Soc.*, *Dalton Trans.*, 1998, 139.

21 M. D. Ward, *Inorg. Chem.*, 1996, **35**, 1712.

22 L. M. Vogler and K. J. Brewer, *Inorg. Chem.*, 1996, **35**, 818.

23 G. A. Crosby and W. H. Elfring, Jr., *J. Phys. Chem.*, 1976, **80**, 2206.

24 R. Alsfasser and R. V. Eldik, *Inorg. Chem.*, 1996, **35**, 628.

25 K. D. Keerthi, B. K. Santra and G. K. Lahiri, *Polyhedron*, 1998, **17**, 1387.

26 A. B. P. Lever, *Inorg. Chem.*, 1990, **29**, 1271.

27 K. J. Takeuchi, M. S. Thompson, D. W. Pipes and T. J. Meyer, *Inorg. Chem.*, 1984, **23**, 1845.

28 R. R. Ruminksi, S. Underwood, K. Vallely and S. J. Smith, *Inorg. Chem.*, 1998, **37**, 6528; A. Gerli, J. Reedijk, M. T. Lakin and A. L. Spek, *Inorg. Chem.*, 1995, **34**, 1836.

29 A. Bharath, B. K. Santra, P. Munshi and G. K. Lahiri, *J. Chem. Soc.*, *Dalton Trans.*, 1998, 2643.

30 R. P. Thummel and S. Chirayil, *Inorg. Chim. Acta*, 1988, **154**, 77.

31 R. Samanta, P. Munshi, B. K. Santra and G. K. Lahiri, *Polyhedron*, 1999, **18**, 995; B. K. Santra and G. K. Lahiri, *J. Chem. Soc.*, *Dalton Trans.*, 1997, 1387.

32 G. K. Lahiri, S. Bhattacharya and A. Chakravorty, *J. Chem. Soc.*, *Dalton Trans.*, 1990, 561; L. S. Kelso, D. A. Reitsma and F. R. Keene, *Inorg. Chem.*, 1996, **35**, 5144.

33 J. C. Dobson, J. H. Helms, P. Doppelt, B. P. Sullivan, W. E. Hatfield and T. J. Meyer, *Inorg. Chem.*, 1989, **28**, 2200; B. Douglas, D. H. McDaniel and J. J. Alexander, *Concepts and Models of Inorganic Chemistry*, Wiley, New York, 1983.

34 S. Goswami, A. R. Chakravarty and A. Chakravorty, *J. Chem. Soc.*, *Chem. Commun.*, 1982, 1288.

35 R. Samanta, P. Munshi, B. K. Santra, N. K. Lokanath, M. A. Sridhar, J. S. Prasad and G. K. Lahiri, *J. Organomet. Chem.*, 1999, **581**, 311.

36 R. G. Wilkins, *The Study of Kinetics and Mechanism of Reactions of Transition Metal Complexes*, Allyn and Bacon, Boston, MA, 1974; R. Hariram, B. K. Santra and G. K. Lahiri, *J. Organomet. Chem.*, 1997, **540**, 155.

37 A. C. T. North, D. C. Phillips and F. S. Mathews, *Acta Crystallogr.*, *Sect. A*, 1968, **24**, 351.

38 G. M. Sheldrick, SHELXTL, Version 5.03, Siemens Analytical X-ray Instruments Inc., Madison, WI, 1997.